PNAS
www.pnas.org

Supplementary Information for

Mechanistic basis of neonatal heart regeneration revealed by transcriptome and histone modification profiling

Zhaoning Wang*, Miao Cui*, Akansha M. Shah, Wenduo Ye, Wei Tan, Yi-Li Min, Giovanni A. Botten, John M. Shelton, Ning Liu, Rhonda Bassel-Duby, and Eric N. Olson**

* These authors contributed equally to this work.

** Corresponding author: Eric N. Olson, Ph.D.
Email: eric.olson@utsouthwestern.edu

This PDF file includes:

Supplementary Information text
Figs. S1 to S5
Table S1
References for SI reference citations

Supplementary Information Text

Supplemental Methods

Neonatal MI. Neonatal mice were anesthetized by hypothermia on an ice bed, as previously described (1-3). Lateral thoracotomy at the fourth intercostal space was performed by blunt dissection of the intercostal muscles after skin incision. A tapered needle attached to a non-absorbable 8-0 suture (PROLENE, Ethicon) was passed through the midventricle below the origin of the LAD coronary artery and tied to induce infarction. The pericardial membrane remained intact after LAD ligation. Myocardial ischemia was indicated by the light pallor of the myocardium below the ligature after suturing. After LAD ligation, neonates were removed from the ice bed, thoracic wall incisions were sutured with a 7-0 non-absorbable suture (PROLENE, Ethicon), and the skin wound closed by using skin adhesive. Sham-operated mice underwent the same procedure involving thoracotomy without LAD ligation.

Histology and Immunohistochemistry. Postnatal mouse hearts were fixed in 4% paraformaledehyde (Electron Microscopy Sciences, 15710) in PBS (Sigma, D8537). For trichrome staining, samples were embedded in paraffin, and sectioned at different levels below the suture (for MI hearts) or comparable levels (for Sham hearts), and stained using Masson's trichrome staining method. For immunostaining, samples were kept in 10% sucrose/PBS overnight and 18% sucrose/PBS solution overnight sequentially, embedded in O.C.T. Compound (Fisher Healthcare, 23730571), and cryosectioned at 10 μm intervals. Before staining, cryosections were air-dried for 30 min at room temperature and fixed with 4% PFA for 20 min. Section slides were then washed twice with PBS and permeabilized with 0.3% Triton X-100 (Fisher Scientific, BP151-500) in PBS for 10 min. Sections were then blocked in 5% goat serum (Sigma, G9023)/3% BSA/0.025% Triton X-100/PBS blocking solution for 1 h and stained with primary antibodies against indicated proteins prepared in blocking solution at 4 °C overnight using the following dilutions: cTnT (Invitrogen,

MA5-12960, 1:200), Vimentin (R&D systems, MAB2105, 5 µg/mL), Ki67 (Abcam, ab15580, 1:500), GFP (Aves Labs, GFP-1020, 1:500), pH3 (Cell Signaling Technology, 9701S, 1:200). Sections were subsequently washed with 0.025% Triton X-100/PBS for three times (5 min for each wash), and incubated with corresponding secondary antibodies conjugated to Alexa Fluor 488, 555 or 647 (Invitrogen) prepared in blocking solution at room temperature for 1.5 h. After secondary antibody incubation, sections were washed with PBS, incubated with Hoechst (Thermo Scientific, 62249, 1:2000) diluted in PBS at room temperature for 10 min, and washed twice with PBS before mounting. Images were obtained using a Zeiss LSM 800 confocal microscope.

RNA *In Situ* Hybridization. Probe DNA sequences were synthesized as gBlocks from IDT and cloned into pCRII-D-TOPO vector using TOPO TA Cloning kit (Invitrogen, 450640). ^{35}S-labelled UTP (Perkin Elmer, NEG039C001MC) were used in the in vitro transcription reaction to synthesize ^{35}S-labelled probes, using MAXIscript SP6/T7 Transcription kit (Invitrogen, AM1322). Antisense and sense probes were transcribed with T7 and SP6 polymerases, respectively. Radio-isotopic in situ hybridization was performed as previously described (4). Probe sequences (antisense) are: Fhl1:

TCACGGAGCATTTTTTGCAGTGGAAGCAGTAGTCGTGCCAGGATTGTCCTTCATAGG
CCACCACACTGGAGCCTTTACCAAACCCGGGCCTCGAGGAGCTGCTAAGCTTCGATT
TTTTCTATAAAGAACCACCACCCACGAGGGACAAGTCCTCTCTCCACCCGGATGCCT
GCCCCGGAGGTTGGCGCTGGGAAACAGGGTGAGAGGCAAGCGTTTCCCGTGGCACA
CTGGGGACTTCCTAGCTTTAGAGACTGGGTGGCTCACTCTTGACACAGTCCTTTTCCC
AGTGATGGGGTTCTTGCATCCAGCACACTTCTTGGCCACAAAGTTCTTGTAGCAATCC
ACGCAGTAATACTGGTCCTCCACAGCGGTGAAACGCTGCCCAGCCAGCTTCTTAGAG
CAGGTAACACACACAAAGCACTCGGCATGCCAGGGCTGATCCTGGTAAGTGATTCCT
CCAGATGTGATGGCCTTGTTGCACTTCACGCAATGTTTGGCGA

Tgm2:

ATGAAGCCCTGTTGCGTAAGGACATATTCCCGTCGCTCCTCCTCTGAGTCTAGGTACA
CATCATCGGCTGGGCACCAGGCATTGTAGAGCAGGATGAAGTGGCCCAGCACAAAG
CTGGAGCCCTGGTAGCCAGTAGAAGCCTCTAGGCTGAGACGGTACAGGCCAATAGG
AGCATTGGCTGGGGTGCAGAGCTGTAGCGAGAGGACATTGTCCTGTTGGTCCAGCAC
TGAGGCTGACCAAGATCCCTCCTCCACATTGTCAGACAGTGAGAAGCGGGCCTTGGT
CCCTGCCTCTTCACTGGGATCTGGGCCGGTCACAGCACCGAACGTGAGGCTGTCCAC
GCTGGCCTCGTAGCCACGGCCCTCGAAGTACAGAGTCAGCCGGAAGCGCTGACCAC
GACGCAGCACCAGTTTCTCTTGGCATAGGTCGGCCGTGTGGTGGTCACGGCCATTGG
CCTGAATCTCCAAATCACACCTCTCCAGGAGCAGCTCCTCTGCCAT

Cardiomyocyte Culture and Proliferation Assay. Neonatal rat ventricular myocytes (NRVMs) were isolated from 1- or 2-day-old Sprague-Dawley rats with the Isolation System for Neonatal Rat/Mouse Cardiomyocytes (Cellutron, nc-6031) according to the manufacturer's instructions. NRVMs were plated at a density of 1.5×10^5 cells/well of gelatin-coated 12-well plates, and were maintained in Dulbecco's modified Eagle's medium (DMEM)/199 medium (3:1) with 3% fetal bovine serum (FBS) and penicillin-streptomycin.

Recombinant CCL24 protein (R&D Systems, 1017-MP-025) and recombinant IGF-2 protein (R&D Systems, 792-MG-050) were reconstituted in 0.1% BSA/PBS. Before recombinant protein treatment, NRVMs were starved in serum-free medium (DMEM/199 medium) for 4 h, and cultured in 0.001% FBS medium (DMEM/199 medium) throughout the experiment. NRVMs were treated with recombinant proteins at indicated final concentration for 24 h, followed by treatment with 10 μM EdU (Lumiprobe, 10540) for an additional 24 h. After that, cells were fixed with 4% PFA at room temperature for 10 min, permeabilized with 0.3% Triton X-100 in PBS, followed by EdU staining by click chemistry (a label mix containing 8 μM sulfo-Cy5-Azide, 2 mM $CuSO_4\cdot5H_2O$, and 20 mg/mL Ascorbic acid in PBS was applied to cells for 30 min). Next, cells were stained with

antibodies against pH3 (Cell Signaling Technology, 9701S, 1:200), Aurora B (Abcam, ab2254, 1:200), and Cardiac Troponin T (Thermo Fisher, MA5-12960,1:200). Cells were washed with 0.025% Triton X-100/PBS for three times and secondary antibody staining was performed as described above. Nuclei were counter-stained with DAPI (Invitrogen, D1306, 1:2000). Imaging was performed on a Keyence BZ-X700 microscope. Five fields at 10x magnification were captured for each well. Quantification was carried out by counting the proportion of $EdU^+/cTnT^+$, $pH3^+/cTnT^+$, or Aurora $B^+/cTnT^+$ cells in $cTnT^+$ cells on immunofluorescent staining images. This value was compared to that of the negative control.

Adenoviruses for YAP1 S112A and 3xFlagHA-Igf2bp3 were generated using the Adeno-X Adenoviral System 3 (Clontech, 632267). The 3xFlagHA-Igf2bp3 adenovirus was generated by cloning mouse Igf2bp3 cDNA with an N-terminal triple FLAG and HA epitope tag into the pAdx-CMV vector containing a ZsGreen1 fluorescent protein. The plasmid was transformed using Stellar competent cells (Clontech, 636763) for homologous recombination. pAdx-CMV-YFP (Clontech) was used as the negative control. Adenoviruses were generated by transfecting linearized recombinant adenoviral plasmids into a mammalian packaging cell line Adeno-X 293. Primary lysates were used to re-infect Adeno-X 293 cells to generate higher-titer viruses. For assessing cardiomyocyte proliferation, 8 μL of the respective adenovirus was transduced into NRVMs per 12-well with serum-free medium (DMEM/199 medium) and cultured for 48 h. For EdU labeling, cells were treated for 12 h with 10 μM EdU (Lumiprobe, 10540). Cells were then fixed with 4% PFA at room temperature for 10 min and permeabilized with 0.3% Triton X-100 in PBS. EdU was detected by click chemistry, nuclei were stained with DAPI, and immunostaining for Cardiac Troponin T (Thermo Fisher, MA5-12960, 1:200), pH3 (Cell Signaling Technology, 9701S, 1:200), and Aurora B (Abcam, ab2254, 1:200) was performed. Imaging was performed on a Keyence BZ-X700 microscope. Five fields at 10x magnification were captured for each well. Quantification was carried out by counting the proportion of $EdU^+/cTnT^+$, $pH3^+/cTnT^+$, or Aurora $B^+/cTnT^+$ cells in

$cTnT^+$ cells on immunofluorescent staining images. This value was compared to that of the negative control.

Chromatin Immunoprecipitation (ChIP). Tissue samples were ground to powder and crosslinked with 2% formaldehyde in PBS for 30 min and quenched with 0.125 M glycine for 10 min at room temperature. Crosslinked samples were then washed with cold PBS and further homogenized with a Dounce tissue grinder. Samples were collected by a brief spin, and treated with 10 mM Tris-HCl (pH 8.0), 10mM NaCl and 0.2% NP-40 for 30 min to collect nuclei. After nuclear extraction, chromatin was sheared on a Bioruptor Pico (Diagenode) for 20 cycles (30 sec on/ 30 sec off for each cycle) at 4°C in sonication buffer (0.1% SDS, 1% Triton X-100, 10 mM Tris-HCl, 1 mM EDTA, 0.1% sodium deoxycholate, 0.25% sarkosyl, 1 mM DTT, 1x cOmplete Protease Inhibitor Cocktail (Roche), and 200 μM PMSF, pH 8.0). After sonication, 1% of the sonicated chromatin from each sample was taken out as "input" samples. The remaining sonicated chromatin was evenly split for H3K27ac or H3K27me3 ChIP. Sonication buffer was added to make the final volume to 1 mL. NaCl was then added to a final concentration of 300 mM for each sample. 1 μg H3K27ac antibody (Diagenode, C15410196) or H3K27me3 (Diagenode, C15410195) was added to each sample and incubated at 4°C overnight with gentle rotation. The next day, 30 μL of pre-washed Dynabeads Protein G (Invitrogen, 10004D) was added to each sample for a two-hour incubation. After that, the beads were washed twice with 1 mL RIPA 0 buffer (0.1% SDS, 1% Triton X-100, 10 mM Tris-HCl, 1 mM EDTA, 0.1% sodium deoxycholate, pH 8.0), twice with 1 mL RIPA 0.3 buffer (0.1% SDS, 1% Triton X-100, 10 mM Tris-HCl, 1 mM EDTA, 0.1% sodium deoxycholate, 300 mM NaCl, pH 8.0), twice with 1 mL LiCl wash buffer (250 mM LiCl, 0.5% IGEPAL CA-630, 0.5% sodium deoxycholate, 1 mM EDTA, 10 mM Tris-HCl, pH 8.0), and finally twice with 1 mL TE buffer (10 mM Tris-HCl, 1 mM EDTA, pH 8.0). For each ChIP sample or input sample, 100 uL of SDS elution buffer (1% SDS, 10 mM EDTA, 50 mM Tris-HCl, pH 8.0) was added and incubation was done at 65°C overnight on a ThermoMixer (Eppendorf) at 1000 rpm.

The next day, supernatant was collected and further treated with 0.5 µg RNaseA (Sigma, 11119915001) for 30 min at 37°C, followed by 20 µg Proteinase K (NEB, P8107S) treatment at 37°C for 2h. DNA was recovered using MinElute PCR Purification Kit (QIAGEN, 28004) according to manufacturer's protocol.

Transgenic Enhancer Assay. Transgenic enhancer assay was performed as previously described (5). Briefly, *Tnni1* enhancer sequence (chr1:135,800,059-135,801,243) was synthesized as a gblock from Integrated DNA Technologies and cloned to pHsp68-LacZ-Gateway vector (Addgene plasmid # 37843), a gift from Nadav Ahituv. Linearized plasmid was used for pronuclear injections of B6C3F1 embryos. Embryos were harvested at 11.5 dpc and dissected in cold PBS, followed by lacZ staining using β-Gal Staining Kit (Invitrogen, K146501) according to manufacturer's protocol.

Transthoracic Echocardiography. Cardiac function was evaluated by two-dimensional transthoracic echocardiography on conscious mice using a VisualSonics Vevo2100 imaging system as described previously (6) . Fractional shortening (FS) and ejection fraction (EF) were used as indices of cardiac contractile function. M-mode tracings were used to measure LV internal diameter at end diastole (LVIDd) and end systole (LVIDs). FS was calculated according to the following formula: FS = [(LVIDd − LVIDs)/LVIDd] × 100%. EF was calculated as EF = (LVEDV-LVESV)/LVEDV × 100%. (LVESV, left ventricular end systolic volume; LVEDV, left ventricular end diastolic volume.) All measurements were performed by an experienced operator blinded to the study.

Quantitative Real-time PCR (qPCR). To assess Igf2bp3 expression after AAV9 injection, total RNA was extracted from ventricles using TRIZOL (Invitrogen, 15596018) according to manufacturer's protocol. cDNA was synthesize using iScript Reverse Transcription Supermix

(Biorad, 1708840). Gene expression was assessed using KAPA SYBR FAST kit (KAPA, KK4605) and quantified using the ddCt method with the following primers:

Igf2bp3-F: TCGAGGCGCTTTCAGGTAAAA

Igf2bp3-R: CTCTGCCGTTTAGGGACCG

18s rRNA-F: GTAACCCGTTGAACCCCATT

18s rRNA-R: CCATCCAATCGGTAGTAGCG

RNA-Seq Data Analysis. Quality control of RNA-Seq data was performed using FastQC Tool (Version 0.11.4). Sequencing reads were aligned to mouse GRCm38 (mm10) reference genome using HiSTAT2 (Version 2.0.4) with default settings and --rna-strandness F (7). Aligned reads were counted using featurecount (Version 1.6.0) per gene ID (8). Differential gene expression analysis was performed with the R package edgeR (Version 3.20.5) using the GLM approach (9). For each comparison, genes with more than 1 CPM (Count Per Million) in at least three samples were considered as expressed and were used for calculating normalization factor. Cutoff values of absolute fold change greater than 2.0 and false discovery rate less than 0.01 were used to select differentially expressed genes between sample group comparisons. Normalized gene CPM values were used to calculate RPKM (Reads Per Kilobase per Million mapped reads) values, which were then used for heatmap plotting. Gene set enrichment analysis (GSEA) was performed using the GSEA software (Version 3.0) (https://www.broadinstitute.org/gsea/) (10). For the hierarchical clustering analysis in Fig. 1*B*, Spearman correlation was performed using the Correlation function from the stat package in R. Clusters were determined from the second branching points of the clustering tree, and P8+7 dps sample was combined with P1+7 dps, P8+3 dps, P1+7 dpi, and P8+1.5 dps samples to form cluster 1, based on high correlation scores among these samples.

ChIP-Seq Data Analysis. ChIP-Seq raw reads were aligned to mouse (mm10) genome assembly using Bowtie2 (Version 2.3.4) with default parameters (11). For H3K27ac samples, duplicated

reads were removed from further analysis. MACS2 (Version 2.1.1) was first applied to each sample to perform peaking calling using the "-nomodel" parameter and was next applied to merged pseudo samples of the biological duplicates (12). Only the peaks that are present in both replicates as well as the merged pseudo sample, defined by at least 50% overlapping of the peak coordinates, were kept as real peaks for further analyses. To compare ChIP-Seq signal intensities between MI and sham samples, diffbind (Version 1.16.3) was applied to calculate the normalized ChIP-Seq enrichment score with summits=250 (13). Cutoff values of absolute fold change greater than 2.0 and false discovery rate less than 0.05 were used for differential peak analysis between sample groups. The normalized peak scores calculated using the TMM function in edgeR were plotted in the heatmaps to show peak intensity across time points. For H3K27me3 samples, duplicates and X-chromosome mapped reads were removed. MACS2 was applied to each biological sample using "--broad-cutoff 0.01 –nomodel" parameter. Diffbind was applied to calculate the differentially bound peak with summits=500. Fold change value of two and FDR less than 0.05 were used as cutoffs.

Encode Data Analysis. The following ENCODE datasets for H3K27ac ChIP-Seq and input control from developing mouse hearts were downloaded from ENCODE portal (https://www.encodeproject.org): ENCSR582SPN, ENCSR681NQF, ENCSR123MLY, ENCSR646GHA, ENCSR360ANE, ENCSR840PFW, ENCSR846PJO, ENCSR685AMF, ENCSR675HDX, ENCSR334IOH, ENCSR000CDF, and ENCSR000CA. The ChIP-Seq reads mapping and peak calling were performed as described above. Differential peak analysis was done between each embryonic time points (E10, E12, E14, and E16) and the 8-week old sample. For each comparison, fold change of 2 with FDR<0.05 was used as cutoffs to get the peaks enriched in the embryonic hearts and peaks enriched in the adult heart. The four resulted peak sets that showed higher intensity in the embryonic samples were then merged to get the consensus developmental peaks.

Transcription Factor Binding Motif Analysis. Differential H3K27ac peaks were first depleted with the annotated promoter sequences (defined as -1kb to +100bp from TSS) to get MI-responsive enhancers. Chromatin regions of these enhancers were searched for known motifs in the JASPAR database (14) using HOMER (Version 4.8) "analyzing genomic positions" function with "-size = 500" (15). Motifs preferentially enriched at each time point and condition were grouped by the time point of the highest –log(P-value). Z-scores of –log(P-value) were ranked and plotted in a heatmap.

Gene Ontology Analysis. Gene ontology analysis of differentially expressed genes from indicated comparisons was performed using Metascape (16). Gene ontology analysis of indicated ChIP-Seq peaks was performed using Genomic Regions Enrichment of Annotations Tool (GREAT, Version 3.0.0) with "Basal plus extension" setting (17).

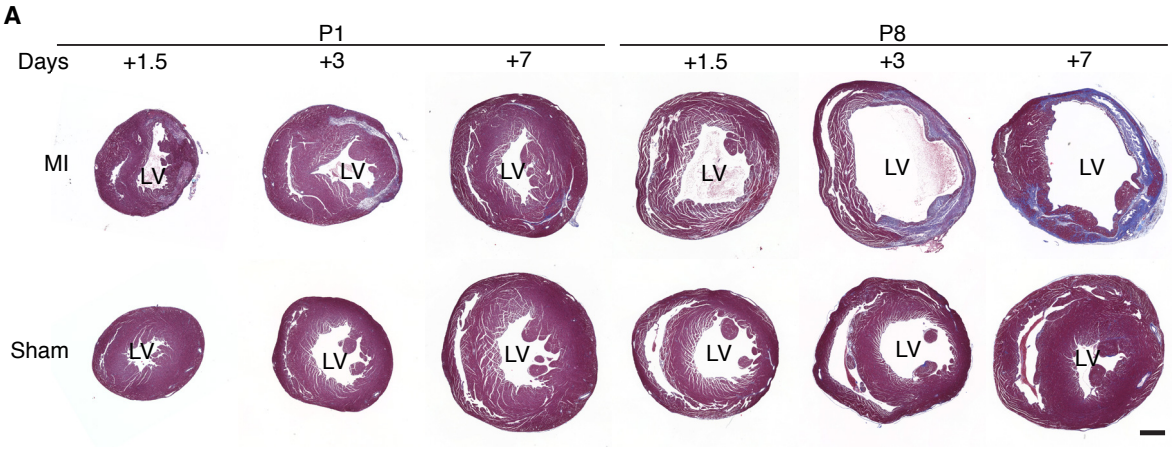

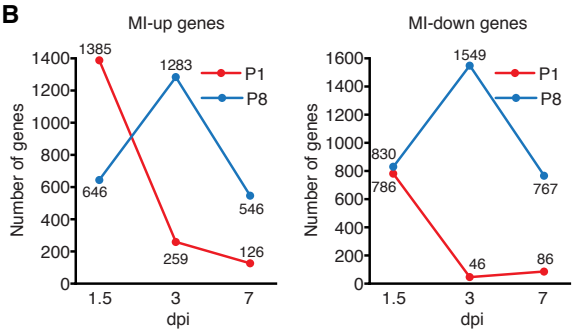

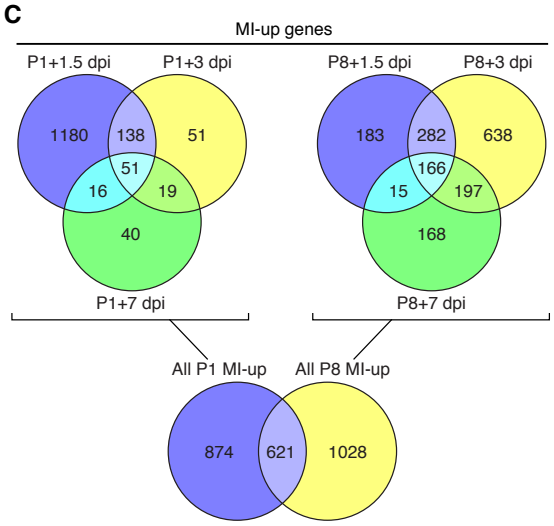

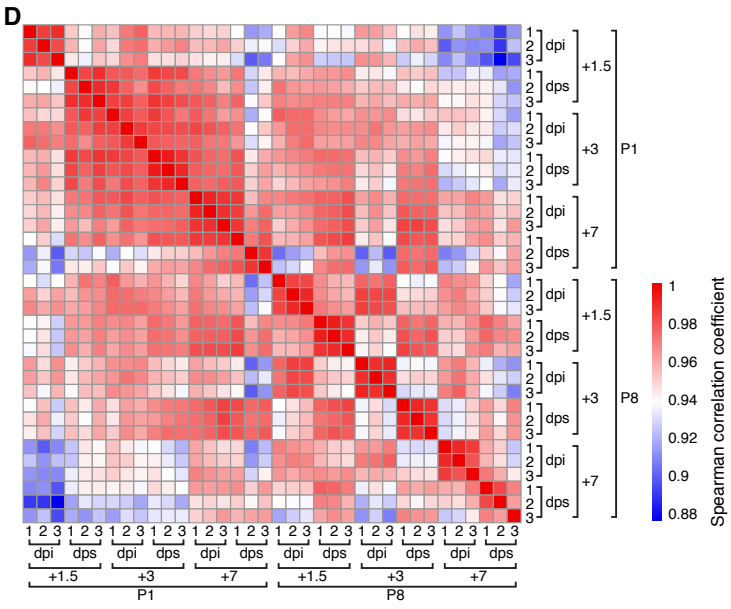

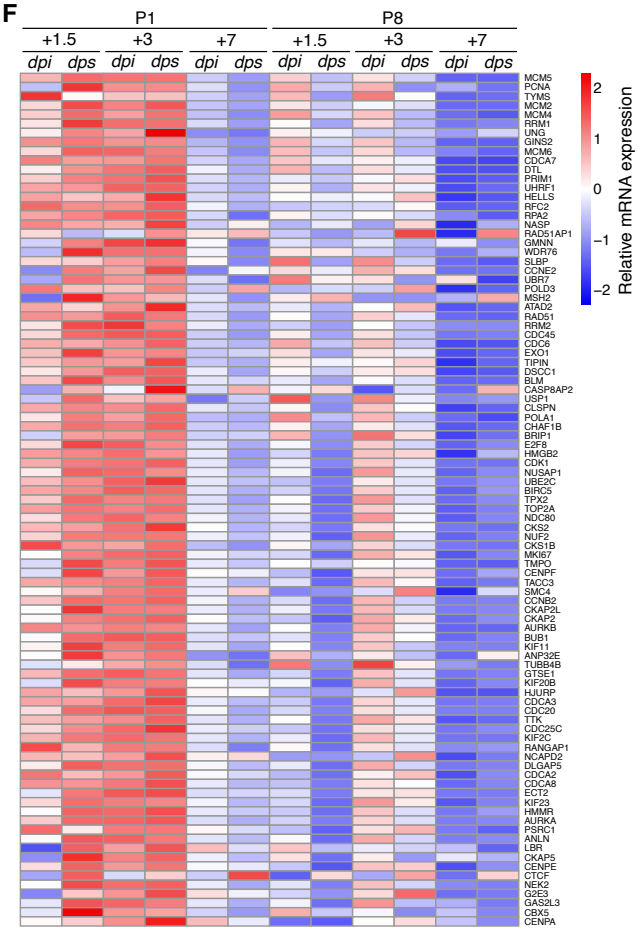

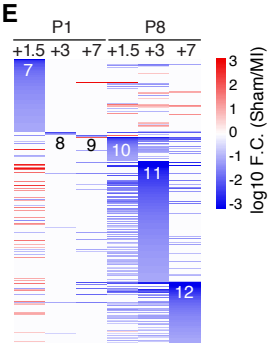

Module (# of genes)	Gene Ontology	-log10 (P-value)
7 (715)	fatty acid metabolic process	13.61
	regulation of heart contraction	10.39
	cardiac conduction	6.75
	tricarboxylic acid cycle	6.06
8 (28)	actin filament organization	2.29
9 (22)	-	-
10 (240)	chloride transport	3.47
	muscle contraction	3.02
11 (1176)	regulation of ion transport	7.58
	regulation of blood circulation	5.09
	artery smooth muscle contraction	3.57
12 (590)	ATP metabolic process	14.22
	oxydative phosphorylation	12.49
	cardiac muscle contraction	2.87

Fig. S1. Histology and transcriptomic profiling of the regenerating and non-regenerating hearts.

(A). Trichrome staining of transverse sections of the P1 and P8 hearts at 1.5, 3, and 7 days post-injury (dpi) and days post-sham (dps). Scale bar, 500 μm.

(B). Number of MI-up and MI-down genes in the P1 and P8 hearts at 1.5, 3, and 7 dpi. Fold change > 2 and FDR < 0.01 were used as cutoffs. Dpi, days post-injury.

(C). Venn diagrams showing numbers of unique or shared MI-up genes in P1 or P8 hearts after injury. Dpi, days post-injury.

(D). Spearman correlation of 36 RNA-Seq datasets showing the data reproducibility. Spearman coefficients over 0.96 were observed among biological triplicates for each timepoint and condition. Dpi, days post-injury; dps, days post-sham.

(E). Left, heatmap showing log10 (Fold Change (F.C.)) of MI-down genes. Right, selected top enriched GO terms for MI-down genes from modules 7 to 12.

(F). Heatmap showing expression level of cell-cycle related genes across all the timepoints and conditions. Dpi. Days post-injury; dps, days post-sham.

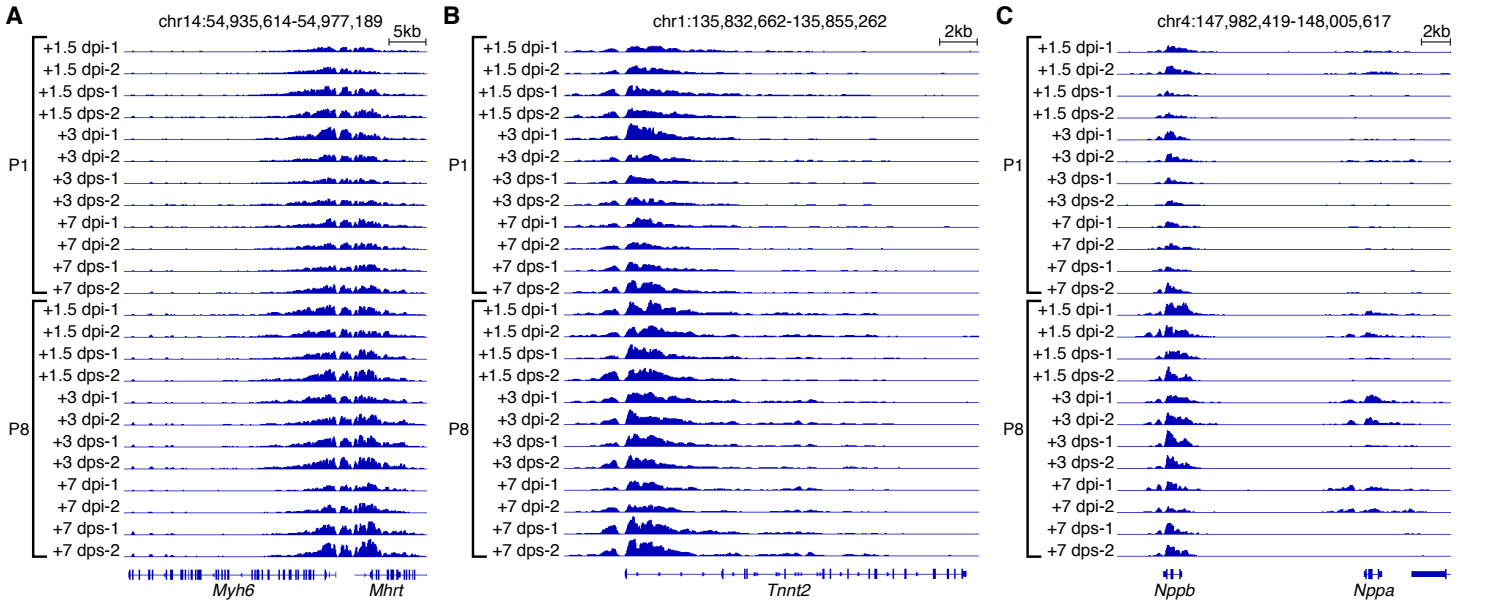

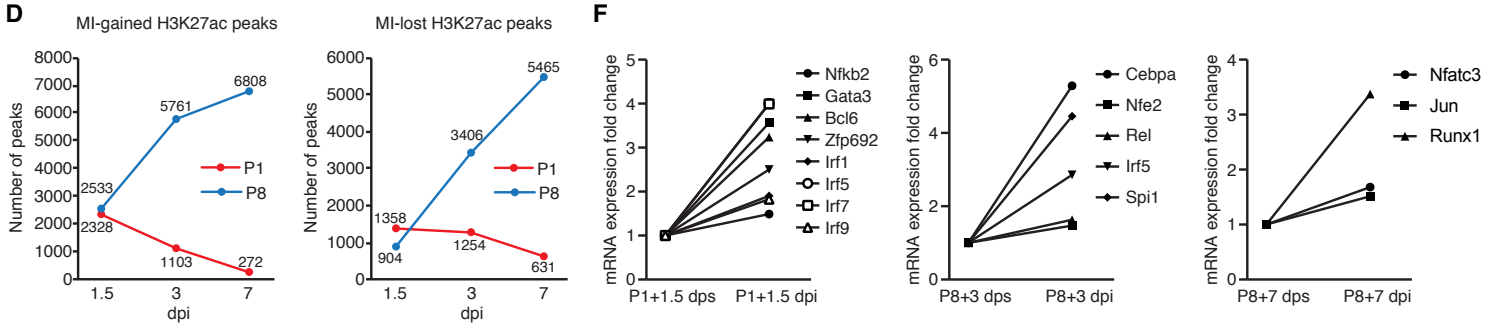

E

	P1+1.5 dpi peaks	P1+3 dpi peaks	P1+7 dpi peaks	P8+1.5 dpi peaks	P8+3 dpi peaks	P8+7 dpi peaks
Target genes being upregulated in MI (p-value for pair-wise t-test)	1.07E-69	4.02E-04	3.18E-01	1.52E-61	2.18E-212	7.76E-208

	P1+1.5 dps peaks	P1+3 dps peaks	P1+7 dps peaks	P8+1.5 dps peaks	P8+3 dps peaks	P8+7 dps peaks
Target genes being downregulated in MI (p-value for pair-wise t-test)	1.46E-68	3.26E-11	9.97E-08	3.28E-06	2.92E-09	4.18E-22

Fig. S2. Examples of H3K27ac tracks and correlation of MI-responsive peak activity and gene expression.

(A). H3K27ac signal tracks at the genomic locus of cardiac marker gene *Myh6* across samples. Dpi, days post-injury; dps, days post-sham.

(B). H3K27ac signal tracks at the genomic locus of cardiac marker gene *Tnnt2* across samples. Dpi, days post-injury; dps, days post-sham.

(C). H3K27ac signal tracks at the genomic locus of known cardiomyopathy genes *Nppa* and *Nppb* across samples. Dpi, days post-injury; dps, days post-sham.

(D). Numbers of MI-gained and MI-lost H3K27ac peaks in the P1 and P8 hearts at 1.5, 3, and 7 days post-injury (dpi). Fold change >2 and FDR < 0.05 were used as cutoff.

(E). Correlation of MI-responsive peak activity to MI-responsive gene expression. For each group of MI-responsive peaks, their nearest gene activities were used in a pairwise t-test to examine correlation between the target gene activity with the peak activity in MI and Sham hearts. For MI-gained H3K27ac peaks, a positive correlation is defined as target gene being induced by MI at the same time point with P-value < 0.05. For MI-lost peaks, a positive correlation is defined as target genes being repressed by MI at the same time point with P-value < 0.05. Dpi, days post-injury.

(F). RNA-Seq data showing MI-up TF motif related genes were up-regulated at corresponding time points. For each TF, the gene expression was normalized to dps samples at the indicated time point.

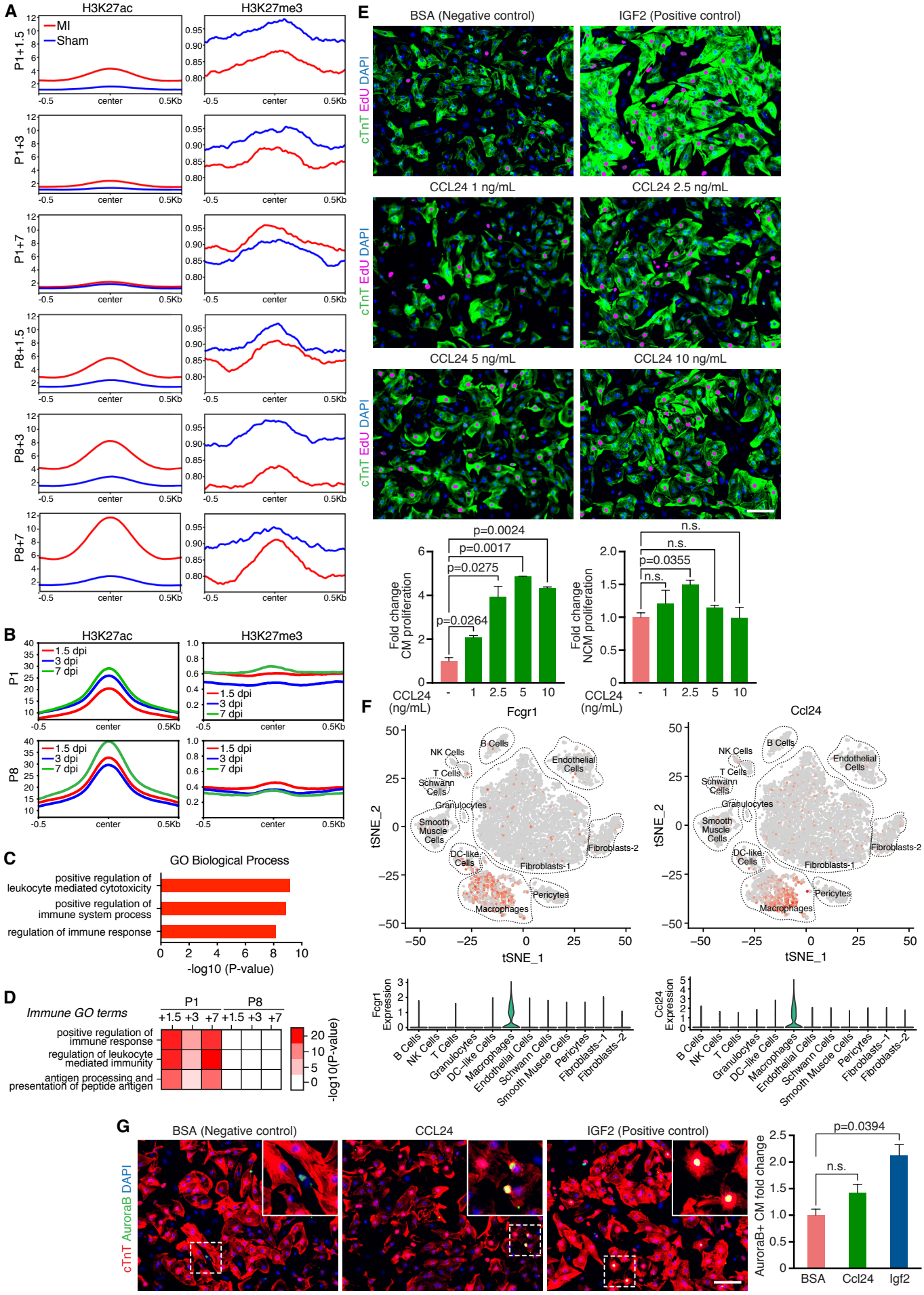
A
H3K27ac
H3K27me3
MI
Sham
P1+1.5
P1+3
P1+7
P8+1.5
P8+3
P8+7
-0.5
center
0.5Kb
B
H3K27ac
H3K27me3
P1
P8
1.5 dpi
3 dpi
7 dpi
C
GO Biological Process
positive regulation of leukocyte mediated cytotoxicity
positive regulation of immune system process
regulation of immune response
-log10 (P-value)
D
Immune GO terms
P1
P8
+1.5 +3 +7 +1.5 +3 +7
positive regulation of immune response
regulation of leukocyte mediated immunity
antigen processing and presentation of peptide antigen
-log10(P-value)
E
BSA (Negative control)
IGF2 (Positive control)
CCL24 1 ng/mL
CCL24 2.5 ng/mL
CCL24 5 ng/mL
CCL24 10 ng/mL
cTnT EdU DAPI
p=0.0024
p=0.0017
p=0.0275
p=0.0264
Fold change CM proliferation
CCL24 (ng/mL)
n.s.
p=0.0355
Fold change NCM proliferation
F
Fcgr1
Ccl24
tSNE_1
tSNE_2
B Cells
NK Cells
T Cells
Schwann Cells
Granulocytes
Smooth Muscle Cells
DC-like Cells
Endothelial Cells
Fibroblasts-1
Fibroblasts-2
Pericytes
Macrophages
Fcgr1 Expression
Ccl24 Expression
G
BSA (Negative control)
CCL24
IGF2 (Positive control)
cTnT AuroraB DAPI
p=0.0394
n.s.
AuroraB+ CM fold change
BSA
Ccl24
Igf2

Fig. S3. Differential immune responses in P1 and P8 hearts.

(A). Metagene plots showing the normalized average signal (Y-axis) of H3K27ac (left) or H3K27me3 (right) at immune response peaks identified in Fig. 3*A*, in both P1 and P8 MI and Sham hearts at each timepoint following injury.

(B). Metagene plots showing the normalized average signal (Y-axis) of H3K27ac (left) and H3K27me3 (right) at control regions, where H3K27ac signals were not induced upon MI. H3K27me3 deposition on these regions were not significantly increased after P1 MI.

(C). GO terms enriched in H3K27me3 bound peak regions identified from Fig. 3*D*.

(D). Heatmap showing -log10 (P-value) of immune-response related GO terms in MI-gained H3K27me3 genomic regions in P1 and P8 heart at each timepoint following injury.

(E). EdU (violet) incorporation and cardiac Troponin T (cTnT) (green) immunostaining of NRVM cells treated with 200 ng/mL BSA (Negative control), 20 ng/mL IGF2 (Positive control), 1 ng/mL CCL24, 2.5 ng/mL CCL24, 5 ng/mL CCL24, or 10 ng/mL CCL24 (upper), with quantification showing the proportion of EdU positive cells among cTnT positive (CM) or negative (NCM) cells (lower) (n=2 for each group). Scale bar, 100 μm.

(F). Ccl24 is specifically expressed by macrophages in the heart. Up, tSNE plots showing the expression of *Fcgr1* (Cd64), a macrophage marker gene, and *Ccl24* among non-CM cell population in the heart. Down, violin plots showing the expression of *Fcgr1* and *Ccl24* expression are specific to macrophage population in the heart. Data source: Skelly et al., 2018 (18).

(G). Left, immunofluorescent staining of cTnT (red), Aurora B (green) proteins on NRVMs treated with 200 ng/mL BSA (negative control), 5 ng/mL CCL24, or 20 ng/mL IGF2 (positive control) recombinant proteins (n=2 for each group). Nuclei were counter-stained with DAPI (blue). Scale bar, 100 μm. Right, fold change of the Aurora $B^+/cTnT^+$ double positive cells proportion in CCL24 or IGF2 treated groups compared with BSA control was calculated.

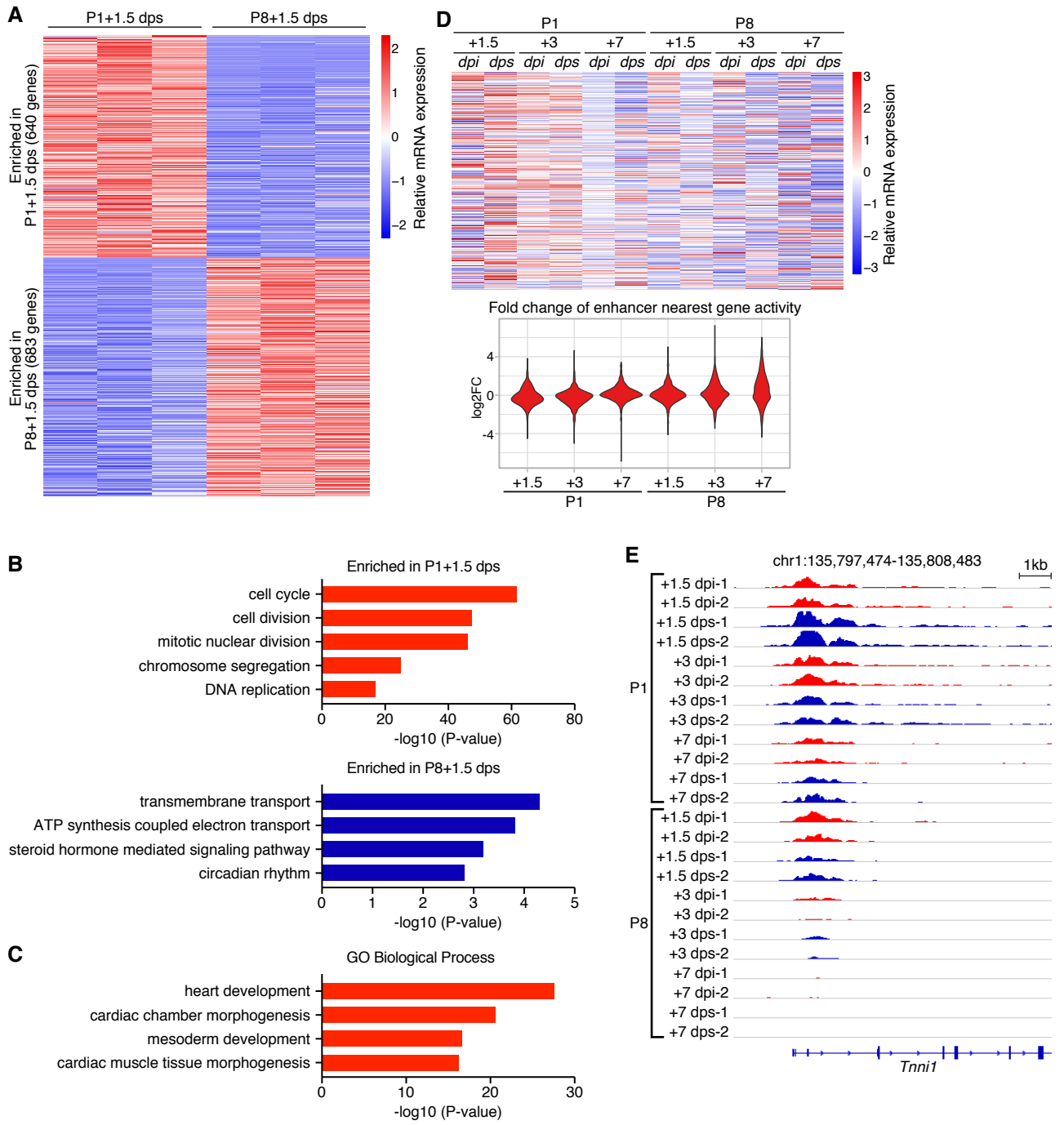
A
P1+1.5 dps
P8+1.5 dps
Enriched in P1+1.5 dps (640 genes)
Enriched in P8+1.5 dps (683 genes)
Relative mRNA expression
D
P1
P8
+1.5
+3
+7
dpi
dps
Relative mRNA expression
Fold change of enhancer nearest gene activity
log2FC
B
Enriched in P1+1.5 dps
cell cycle
cell division
mitotic nuclear division
chromosome segregation
DNA replication
-log10 (P-value)
Enriched in P8+1.5 dps
transmembrane transport
ATP synthesis coupled electron transport
steroid hormone mediated signaling pathway
circadian rhythm
-log10 (P-value)
C
GO Biological Process
heart development
cardiac chamber morphogenesis
mesoderm development
cardiac muscle tissue morphogenesis
-log10 (P-value)
E
chr1:135,797,474-135,808,483
1kb
+1.5 dpi-1
+1.5 dpi-2
+1.5 dps-1
+1.5 dps-2
+3 dpi-1
+3 dpi-2
+3 dps-1
+3 dps-2
+7 dpi-1
+7 dpi-2
+7 dps-1
+7 dps-2
P1
P8
Tnni1

Fig. S4. Retention of cell cycle and embryonic developmental gene programs in neonatal hearts.

(A). Heatmap showing relative expression levels of differentially expressed genes in P1+1.5 days post-sham (dps) and P8+1.5 dps hearts.

(B). GO terms enriched in P1+1.5 dps hearts (up) and P8+1.5 dps hearts (down).

(C). GO terms enriched in H3K27ac peak regions identified from Fig. 4*B*.

(D). Upper, heatmap showing expression of developmental H3K27ac peak nearest genes. Lower, violin plot showing log2 (Fold Change (F.C.)) of developmental H3K27ac peak nearest genes. The log2 (Fold Change) for the majority of the genes is around zero, indicating they are not induced upon MI.

(E). H3K27ac ChIP-Seq signal tracks at the gene Tnni1 locus across all timepoints following injury in P1 and P8 hearts. Signal tracks from post-injury hearts are highlighted in red, and signal tracks from post-sham hearts are in blue. Dpi, days post-injury; dps, days post-sham.

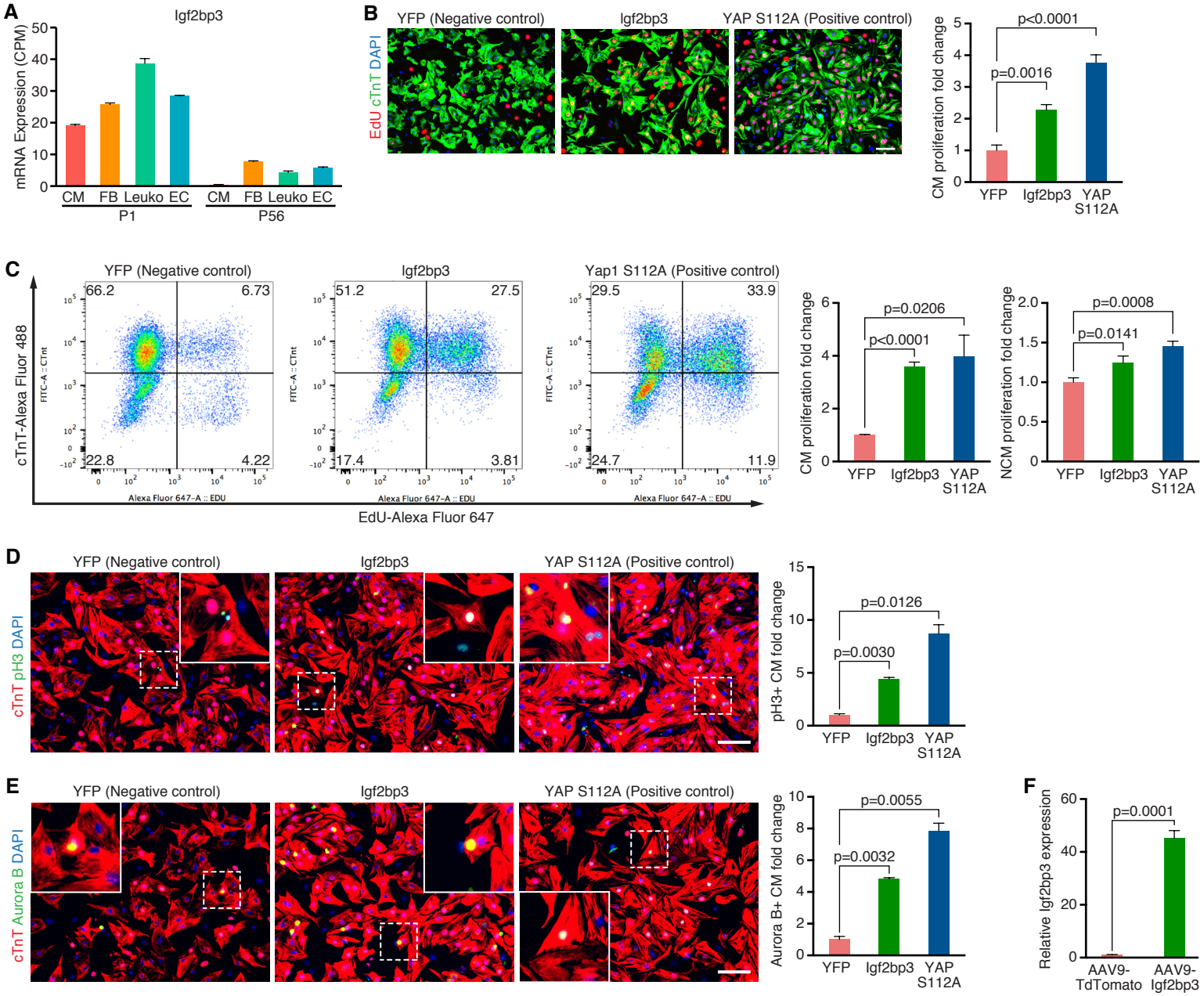
A
Igf2bp3
mRNA Expression (CPM)
CM FB Leuko EC
P1
CM FB Leuko EC
P56
B
YFP (Negative control)
Igf2bp3
YAP S112A (Positive control)
EdU cTnT DAPI
CM proliferation fold change
p<0.0001
p=0.0016
YFP
Igf2bp3
YAP S112A
C
YFP (Negative control)
Igf2bp3
Yap1 S112A (Positive control)
cTnT-Alexa Fluor 488
EdU-Alexa Fluor 647
66.2
6.73
22.8
4.22
51.2
27.5
17.4
3.81
29.5
33.9
24.7
11.9
CM proliferation fold change
p=0.0206
p<0.0001
NCM proliferation fold change
p=0.0008
p=0.0141
D
YFP (Negative control)
Igf2bp3
YAP S112A (Positive control)
cTnT pH3 DAPI
pH3+ CM fold change
p=0.0126
p=0.0030
E
YFP (Negative control)
Igf2bp3
YAP S112A (Positive control)
cTnT Aurora B DAPI
Aurora B+ CM fold change
p=0.0055
p=0.0032
F
Relative Igf2bp3 expression
p=0.0001
AAV9-TdTomato
AAV9-Igf2bp3

Fig. S5. Igf2bp3 promotes cardiomyocyte proliferation.

(A). Igf2bp3 is expressed in multiple cardiac cell lineages including CMs. Data source: Quaife-Ryan et al., 2017 (19).

(B). EdU incorporation and cardiac Troponin T (cTnT) immunostaining of NRVM cells overexpressing YFP (negative control), Igf2bp3, or YAP S112A (positive control) using adenoviral delivery(left), with quantification showing the proportion of EdU positive cells among cTnT positive cells (right, n=4 for each group). Scale bar, 50 μm.

(C). Left, representative flow cytometry plots of NRVM proliferation assay. NRVMs were treated with adenovirus expressing YFP (Negative control), Igf2bp3, or YAP S112A (Positive control), pulse-labelled with EdU (signal intensity on x-axis), co-stained for cardiac Troponin T (cTnT) (signal intensity on y-axis), and analyzed by flow cytometry. Number on each quadrant represents the percentage of cells within. Right, quantification showing the proportion of EdU positive cells among cTnT positive (CM) or negative (NCM) cells (n=3 for each group).

(D). Left, immunofluorescent staining of cTnT (red) and pH3 (green) proteins on NRVMs infected with YFP (Negative control), Igf2bp3, or YAP S112A (Positive control) adenovirus (n=2 for each group). Nuclei were counter-stained with DAPI (blue). Scale bar, 100 μm. Right, fold change of the $pH3^{+}/cTnT^{+}$ double positive cells proportion in Igf2bp3 or YAP S112A infected groups compared with YFP control was calculated.

(E). Left, immunofluorescent staining of cTnT (red) and Aurora B (green) proteins on NRVMs infected with YFP (Negative control), Igf2bp3, or YAP S112A (Positive control) adenovirus (n=2 for each group). Nuclei were counter-stained with DAPI (blue). Scale bar, 100 μm. Right, fold change of the Aurora $B^{+}/cTnT^{+}$ double positive cells proportion in Igf2bp3 or YAP S112A infected groups compared with YFP control was calculated.

(F). Quantitative real-time PCR showing Igf2bp3 is significantly overexpressed in ventricles from mice injected with AAV9-Igf2bp3, compared with AAV9-TdTomato. Mice were injected with AAV9 at P5 and mRNA was analyzed at P8 (n=3 for each group).

Table S1. List of developmental enhancer nearest genes with enriched expression in neonatal heart.

2810408I11Rik	Dgkk	Nfe2l3
Abca4	Diaph3	Nrk
Adamtsl1	Ect2	P3h2
Aldh1b1	Fam83d	P4ha3
Armcx4	H19	Palm2
Aurkb	Hand1	Pbk
Bend4	Hey2	Pdk3
Bex1	Hunk	Prrx2
Bex4	Igf2bp1	Ror2
Bmp7	Igf2bp2	Slc7a5
Cacng6	Igf2bp3	Smarca1
Capn3	Il23a	Sntb1
Ccna2	Kif18b	Soga1
Ccnjl	Kif26b	Sphkap
Cdc25c	Kif4	Sqle
Cdh3	Lmnb1	Srebf2
Cdk1	Lpar3	Stil
Cenpf	Mbnl3	Tead2
Cep55	Mdfi	Tmem26
Cks2	Mxd3	Tnni1
Clcn5	Myoz1	Tspan18
Cma1	Nanog	Tubb6
Col12a1	Ncam1	Uchl1
Ddc	Ncs1	Usp29
Ddr1	Nespas	Vash2

References

1. Mahmoud AI, Porrello ER, Kimura W, Olson EN, & Sadek HA (2014) Surgical models for cardiac regeneration in neonatal mice. *Nat Protoc* 9:305.
2. Porrello ER, *et al.* (2011) Transient regenerative potential of the neonatal mouse heart. *Science* 331(6020):1078-1080.
3. Porrello ER, *et al.* (2013) Regulation of neonatal and adult mammalian heart regeneration by the miR-15 family. *Proc Natl Acad Sci U S A* 110(1):187-192.
4. Shelton JM, Lee MH, Richardson JA, & Patel SB (2000) Microsomal triglyceride transfer protein expression during mouse development. *J Lipid Res* 41(4):532-537.
5. Liu N, *et al.* (2007) An intragenic MEF2-dependent enhancer directs muscle-specific expression of microRNAs 1 and 133. *Proc Natl Acad Sci U S A* 104(52):20844-20849.
6. Song J, *et al.* (2012) Neuronal circuitry mechanism regulating adult quiescent neural stem-cell fate decision. *Nature* 489(7414):150-154.
7. Kim D, Langmead B, & Salzberg SL (2015) HISAT: a fast spliced aligner with low memory requirements. *Nat Methods* 12(4):357-360.
8. Liao Y, Smyth GK, & Shi W (2014) featureCounts: an efficient general purpose program for assigning sequence reads to genomic features. *Bioinformatics* 30(7):923-930.
9. Robinson MD, McCarthy DJ, & Smyth GK (2010) edgeR: a Bioconductor package for differential expression analysis of digital gene expression data. *Bioinformatics* 26(1):139-140.
10. Subramanian A, *et al.* (2005) Gene set enrichment analysis: a knowledge-based approach for interpreting genome-wide expression profiles. *Proc Natl Acad Sci U S A* 102(43):15545-15550.
11. Langmead B & Salzberg SL (2012) Fast gapped-read alignment with Bowtie 2. *Nat Methods* 9(4):357-359.
12. Zhang Y, *et al.* (2008) Model-based analysis of ChIP-Seq (MACS). *Genome Biol* 9(9):R137.
13. Ross-Innes CS, *et al.* (2012) Differential oestrogen receptor binding is associated with clinical outcome in breast cancer. *Nature* 481(7381):389-393.
14. Khan A, *et al.* (2018) JASPAR 2018: update of the open-access database of transcription factor binding profiles and its web framework. *Nucleic Acids Res* 46(D1):D1284.
15. Heinz S, *et al.* (2010) Simple combinations of lineage-determining transcription factors prime cis-regulatory elements required for macrophage and B cell identities. *Mol Cell* 38(4):576-589.
16. Zhou Y, *et al.* (2019) Metascape provides a biologist-oriented resource for the analysis of systems-level datasets. *Nature communications* 10(1):1523.
17. McLean CY, *et al.* (2010) GREAT improves functional interpretation of cis-regulatory regions. *Nat Biotechnol* 28(5):495-501.
18. Skelly DA, *et al.* (2018) Single-Cell Transcriptional Profiling Reveals Cellular Diversity and Intercommunication in the Mouse Heart. *Cell Rep* 22(3):600-610.
19. Quaife-Ryan GA, *et al.* (2017) Multicellular Transcriptional Analysis of Mammalian Heart Regeneration. *Circulation* 136(12):1123-1139.